Sustained SREBP-1 Activation Mediates Cardiac Lipotoxicity to Statins Therapy in Diabetic Mice

Weibin Cai

caiwb@mail.sysu.edu.cn

Sun Yat-sen University https://orcid.org/0000-0003-0934-4507

Tongsheng Huang

Sun Yat-sen University https://orcid.org/0000-0002-7944-5242

Teng Wu

Sun Yat-sen University

Xinlu Fu

Sun Yat-sen University

Honglin Ren

Sun Yat-sen University

Xiaodan He

Sun Yat-sen University

Dinghao Zheng

The Second Xiangya Hospital of Central South University

Jing Tan

Zhongshan Medical School, Sun Yat-sen University

shi Xiong

Sun Yat-sen University

Jiang Qian

Sun Yat-sen University

Yan Zou

Sun Yat-sen University

Huiting Zheng

Sun Yat-sen University

Yuanjun Ji

Sun Yat-sen University

Mengying Liu

Sun Yat-sen University

Yandi Wu

Sun Yat-sen University https://orcid.org/0000-0002-9380-4109

Xing Li
Sun Yat-sen University
Hui Li
Sun Yat-sen University
Li Yan
Sun Yat-Sen University , Guangzhou, China
Meng Ren
Sun Yat-sen Memorial Hospital of Sun Yat-sen University https://orcid.org/0000-0001-9935-1449

Article

Keywords: Sterol regulatory element-binding protein 1, Type 2 diabetes mellitus, Cardiac lipotoxicity, Statins

Posted Date: December 13th, 2023

DOI: https://doi.org/10.21203/rs.3.rs-3724119/v1

Additional Declarations: There is **NO** Competing Interest.

Abstract

Under diabetes conditions, sterol regulatory element-binding protein 1 (SREBP1) activation could cause lipid dysfunction, leading to cardiac lipotoxicity. Here, we sought to investigate the effects of long-term statins use on cardiac lipid accumulation in diabetes and to elucidate whether the potential mechanism is related to SREBP1. Surprisingly, in three kinds of preclinical diabetic mouse model, long-term statins treatment induced cardiac dysfunction in diabetic mice, via accelerated fibrosis and inflammation. We confirmed that endogenous fatty acids (FA) synthesis in cardiomyocytes was increased by ^{13}C-glucose metabolic flux analysis in vitro, and increased lipid deposition in the myocardium. Mechanistically, statins-induced increased cardiac glucose accumulation, further promoted N-glycosylation of SREBP1 cleavage-activating protein (SCAP). Glycosylation stabilized SCAP and reduced its association with insulin-induced gene 1(Insig1), allowing movement of SCAP/SREBP1 to the Golgi and consequent proteolytic activation of SREBP1. Genetic knockdown or L-carnitine inhibition of SREBP1 alleviated statins-induced cardiac dysfunction in diabetic mice. Collectively, these results suggest long-term statins therapy was associated with diabetes myocardial lipotoxicity. This effect was mediated through sustained SREBP-1 activation mediates cardiac endogenous fatty acid synthesis.

Introduction

Patients with type 2 diabetes mellitus (T2DM) are vulnerable to the development of heart failure, which is a major cause of morbidity and mortality[1]. Among diabetic adults, the excess cardiovascular disease (CVD) mortality rate associated with T2DM patients was 2.3 CVD deaths per 1,000[2]. Current evidence indicates that dyslipidemia is a strong risk factor for CVDs inT2DM patients. A meta-analysis demonstrated a 9% proportional reduction in all-cause mortality per mmol/L reduction in low-density lipoprotein cholesterol (LDL-C) in participants with diabetes[3]. Therefore, almost all clinical guidelines strongly recommend lipid-lowering therapy as the first-line treatment for reducing the risk of CVDs in patients with T2DM, especially statins, which are the first-choice for lowering cholesterol levels[4]. Numerous clinical trials have demonstrated that statins therapy can reduce the risk of major cardiovascular events in diabetic patients[5 6,7]. Among patients with T2DM, the incidence of cardiovascular events was not lower among those who received pemafibrate, although pemafibrate lowered triglyceride, VLDL cholesterol, remnant cholesterol, and apolipoprotein C-III levels[8]. Coincidentally, long-term fenofibrate therapy on cardiovascular events in people with T2DM showed no significant decrease in cardiovascular risk, although serum lipid levels were significantly lower [6,9]. Thus, it is puzzling that recent effort at modulating LDL-C levels have failed to reduce residual cardiovascular risk. It is urgent and pivotal to understand the precise mechanism of cardiac lipotoxicity and develop new therapeutic strategies for individuals with T2DM reduce cardiovascular risk.

Statins can increase insulin resistance (IR) in peripheral tissues in individuals without T2DM[1], which has caused statins therapy for reducing cardiovascular risk to remain controversial. Especially in the diabetic heart where insulin sensitivity is seriously disturbed, whether long-term statins therapy will aggravate

cardiac IR effect and further disturb the homeostasis of cardiac metabolic effect remains unclear. Recently, a study reveals that systemic PCSK9 deficiency reduced LDL-cholesterol levels but results in heart failure associated with increased cardiac accumulation of lipid droplets (LDs)[10]. Consistently, in our previous studies, we also found that chronic administration of statins can significantly reduce serum lipid levels but increase kidney accumulation of LDs in diabetic mice, leading to the progression of diabetic nephropathy[11]. Thus, we extend this line of evidence hypothesized that, although high-intensity lipid-lowering therapy can reduce blood lipids, it cannot effectively correct the metabolic disorder in cardiomyocytes caused by diabetes, especially for lipid deposition in the myocardium, so it cannot effectively reduce cardiovascular risk.

To test this hypothesis directly and address this challenge, in this study, we conducted a cross-sectional study to investigate the outcomes of statins administration in diabetic patients, using human heart samples, genetic mouse models and in vitro studies to mimic the clinical situation of long-term statins therapy for diabetes, and to further gain insights into the mechanisms. Here, we show that long-term statins therapy for diabetes led to cardiac dysfunction, which is associated with sustained SREBP-1 activation mediates cardiac lipotoxicity. This may explain why diabetic patients undergoing statins therapy may fail to reduce cardiovascular risk.

Results

SREBP1 is significantly up-regulated in diabetic myocardium and may be associated lipid accumulation.

We found that *db/db* mice began to develop significant hyperlipidemia in the early stage of diabetes (Fig. 1A). The damage of hyperlipidemia to organs is mainly reflected in the ectopic deposition of lipid in organs, resulting in lipotoxicity. Especially for diabetes, cardiac lipotoxicity is one of the important causes of cardiovascular events [12]. Therefore, we used transmission electron microscopy (TEM) and oil red O staining to detect the lipid content of the heart tissue of the mice. As shown in Fig. 1B-C, the heart of *db/db* mice showed a large accumulation of lipid droplets. According to previous research reports, prevention of cardiac lipid accumulation by inhibiting cardiac SREBP activation may be an effective strategy to prevent cardiac lipotoxicity[13]. However, the role of SREBP1 in diabetic heart lipid accumulation is not clear. Next, we examined the expression of SREBP1 in the heart. We found that the expression of SREBP1 was significantly up-regulated in the heart of *db/db* mice (Fig. 1D-G). We used immunofluorescence to detect the expression of SREBP1 and lipid content (Nile red staining) in the heart. We found that lipid accumulation was accompanied by a significant activation of SREBP1 (Fig. 1H). Collectively, SREBP1 is significantly up-regulated in diabetic myocardium and may be associated lipid accumulation.

SREBP1 expression positively correlated with the cardiac dysfunction in human heart specimens

To further confirm that the same metabolic pathways as *db/db* mouse hearts also exist in the human heart, we then used human heart specimens to analyze the correlation between SREBP1 and cardiac dysfunction. Heart specimens from two categories of decedents (normal and T2DM patients) who were age and sex matched were then collected (Supplementary Table 1). T2DM patients presented the most severe glycogen deposition and cardiac fibrosis, as well as higher expression of both SREBP1 and 4-HNE compared with those of normal groups (Fig. 2A-H). Linear regression analysis of the 22 heart specimens revealed that the glycogen content significantly correlated with SREBP1 expression (Fig. 2I). Additionally, SREBP1 expression was significantly correlated with the extent of cardiac fibrosis (Fig. 2J), 4-HNE expression (Fig. 2K). Taken together, these data provided profound evidence that, under the pathological conditions of T2DM, aberrant expression of SREBP1 correlated with glycogen deposition and fibrosis, lipid peroxidation in human hearts.

Long-term statins administration worsens cardiac dysfunction and pathological remodeling in type 2 diabetic mice

In order to treat hyperlipidemia and lipotoxicity of target organs, the current clinical basic lipid-lowering drugs are statins. However, the effect of long-term administration of statins on cardiac lipids and cardiac function in diabetes is not yet clear. In a 40 weeks treatment period, we selected atorvastatin and rosuvastatin, the first-line clinically lipid-lowering drugs, as a representative drug to treat three classic diabetic mice on a daily basis (Fig. 3A). After 40 weeks of statins administration, we evaluated cardiac function in each group of *db/db* mice by echocardiography. In the statins-treated group, both the ejection fraction and fractional shortening were significantly decreased compared with those in the Db group (Fig. 3B to D, Supplementary Table 1). We observed that serum BNP level was also significantly increased after statins treatment (Fig. 3E), which is an important cardiac test in diagnosing heart failure[14].

To further examine the functional status of cardiomyocytes in *db/db* mice and statins-treated *db/db* mice, we subjected freshly isolated primary cardiomyocytes from *db/m*, *db/db* and Db + ATO group mice to a single-cell contraction assay using an electrical stimulator (Fig. 3F-I to VI). We found that the sarcomere shortening trace and sarcomere peak shortening of isolated cardiomyocytes had a similar trend to the ejection fraction in vivo, suggesting that the contraction of isolated cardiomyocytes measured ex vivo responded to the ejection fraction in vivo (Fig. 3F-II). Notably, although there was no significant difference in resting sarcomere length between the three groups of mouse cardiomyocytes, Db + ATO group cardiomyocytes exhibited lower levels of sarcomere shortening (Fig. 3F-II), together with a lower velocity during both the contraction (decreased by 15.8%) and relaxation (decreased by 17.6%) phases (Fig. 3F- III to IV) compared with those of *db/db* mouse cardiomyocytes. Figure 3F-V to VI also reflect further diminished contractility in cardiomyocytes in the Db + ATO group.

Next, we assessed myocardial pathological remodeling, which are often associated with diastolic and systolic dysfunction. Histopathologic analysis of the myocardial tissue revealed cardiomyocyte cell

degeneration and inflammatory infiltrates (Fig. 3G). Employing TEM, hearts from control animals showed a typical myofibrillar arrangement, while cardiomyocyte degeneration was observed in *db/db* mice, especially in the statins-treated *db/db* mice (Fig. 3H). Almost all myofibril constituents were affected, with an evident lack of myofibril integrity disarray and even more serious myofibril breakage, lysis and necrosis. Additionally, mitochondria were swollen and underwent cristolysis, that is, the lysis and breakage of mitochondrial cristae. Mitochondrial disposition was also altered, while *db/m* control mice showed an organized arrangement and mitochondria were clearly visible, with a normal round shape, but *db/db* mice administered statins displayed large accumulations of mitochondria throughout the whole cell, and several were degenerated[15]. Taken together, these findings suggest that statins administration significantly worsens both the contractile and relaxation functions of cardiomyocytes in statins-treated *db/db* mice.

Simultaneously, HE, PAS and Masson staining showed no significant pathological changes in the hearts of *db/m* mice after long-term statins administration (Supplementary Fig. 1A - c). Moreover, we observed the same heart pathological changes in KK-ay diabetic mice and STZ-induced diabetic mice (Supplementary Fig. 2A-D). These results suggested that long-term statins administration worsens cardiac dysfunction and pathological remodeling in type 2 diabetic mice, but not in *db/m* control mice.

Interestingly, from the above results, we observed that the statins-treated *db/db* mice exhibited hallmarks of myocardial functional damage, including progressive reductions in relaxation and contractility recorded by echocardiography, and single-cell contraction assays. Next, we explored the cardiac structural changes in *db/db* mice. As shown in Supplementary Fig. 3A to B and 3 F, we quantified CD68-positive macrophage and interleukin (IL)-1 beta expression in the myocardium. CD68-positive macrophage invasion and IL-1 beta are inflammatory inducers in cardiac disease. We found that CD68-positive macrophages invasion and IL-1 beta expression significantly increased in the statins-treated *db/db* mice. In addition to inflammation, cardiac fibrotic remodeling is also relevant cardiac structural change. We found that statins treatment in *db/db* mice significantly promoted cardiac interstitial fibrosis (Supplementary Fig. 3C to E, G to I). Collectively, long-term statins treatment induces cardiac structural changes in *db/db* mice.

Statins decreased serum cholesterol and LDL-C but were associated with diabetes progression in T2DM

In order to further explore the effect of statins on diabetes, we conducted a small-scale retrospective clinical study. The lipid profile and other clinical characteristics of outcomes of T2DM (n = 291) and T2DM treated with statins (n = 108) are shown in Supplementary Table 3. Statins users had filled prescriptions for statins for a mean duration of 4.34 years. Statins users showed significantly lower serum levels of total cholesterol and LDL-C than those in the control group (Supplementary Table 3). At the same time, we observed a significant decrease in AST in statins users, but did not observe an appreciable change in appreciably for renal function and echocardiography. Interestingly, we found that statins users had significantly increased diabetes indicators such as OGTT-2 h, HbA1c, and fasting C-

peptide levels, which means that statins use increases IR in type 2 diabetes. Our results are also consistent with several RCTs[5,16], observational studies[17], and animal studies[18]. IR has been shown to increase the risk of diabetic complications, and long-term statins administration has been shown to accelerate the progression of diabetic nephropathy in diabetic mice by increasing IR in our previous study[11]. With the advancement of diabetes treatment technology, previously hidden cardiovascular complications have gradually become the main cause of death in diabetes. Therefore, more attention needs to be paid to the effects of long-term statins therapy on diabetes-related cardiac insufficiency. Although this retrospective study found that statins therapy appeared to have no significant effect on echocardiography ($P > 0.05$), but we observed a significant increase in creatine kinase (CK) and high-sensitivity cardiac troponin (hs-cTnT) in statins users (Supplementary Table 3). Elevated hs-TnT and CK is strongly associated with progressive myocardial damage[19,20], which is more sensitive than echocardiography in detecting myocardial injury. These findings suggest that statins use was associated with an increased risk of IR and a higher risk of diabetes progression, especially myocardial injury.

Statins-induced cardiac lipid metabolism disorder contributes to cardiac dysfunction, in which the SREBP lipogenesis pathway plays an important role

Of particular interest for our focus is what the factors are that cause cardiac dysfunction. We therefore hypothesized that statins altered cardiac metabolic effects in *db/db* mice. To address this, indirect calorimetry was performed after *db/db* mice had been on statins treatment for 40 weeks. There was a marked decrease in the respiratory exchange ratio (RER) in statins-treated *db/db* mice, calculated by the ratio of VO_2/VCO_2, compared with *db/db* and *db/m* control mice during the light or the dark cycle (Fig. 4A), indicating a change in the energy source from carbohydrates to proteins and lipids in the mice. In addition to the RER, the energy expenditure, energy balance, food consumed, and water consumed all showed obvious differences (Supplementary Fig. 4A to G). It suggests that statins may mainly alter cardiac lipid metabolism in *db/db* mice. Next, we evaluated the expression of fatty acid metabolism-related genes, including fatty acid uptake, fatty acid oxidation (FAO), and synthesis. Interestingly, we observed that the genes involved in lipolysis, fatty acid uptake and FAO were not significantly changed, while the SREBP1 lipogenesis pathway was significantly upregulated (Fig. 4B-C), highlighting that statins-induced cardiac dysfunction may be associated with the SREBP1 lipogenesis pathway.

Next, we investigated SREBP1 expression and localization in the heart. Consistent with the immunoblot results, we found that SREBP1-N was significantly upregulated and translocated to the nucleus in the myocardium of statins-treated *db/db* mice (Fig. 4D). SREBP1 and its downstream targeting enzymes such as acetyl coenzyme A carboxylase 1(ACC1), were also significantly upregulated in the myocardium of statins-treated *db/db* mice (Fig. 4E to H), which is consistent with western blotting results. Although SREBP1 as a principal transcription factor that regulate the expression of genes involved in FA synthesis[21], but the role of endogenously synthesized FA in cardiomyocyte is unknown, one of the most important questions is whether cardiomyocyte can synthesize FA. Therefore, we focus on whether

Atorvastatin can increase the synthesis of fatty acids in cardiomyocytes under the high-glucose condition.

Because it is difficult to verify lipid synthesis in cardiomyocytes in vivo, we used neonatal mouse primary cardiomyocytes (NMPCs) to verify in vitro whether statins treatment promotes increased lipids synthesis in cardiomyocytes under high glucose conditions. We next traced the metabolic fluxes in statins induced NMPCs and observed generally increased intermediates in fatty acid de novo synthesis pathways (Fig. 5A), further confirming that statins treatment promotes increased the de novo synthesis of FA in cardiomyocytes under high-glucose conditions. Taken together, these results indicate that statins caused cardiac dysfunction through endogenously synthesized FA, in which the SREBP lipogenesis pathway plays an important role.

Genetic knockdown of SREBP1 alleviated statins-induced cardiac dysfunction in diabetic mice

Endogenous FA Synthesis may drive cardiac lipid accumulation. Oil red O staining and electron microscopy analysis also confirmed that statins caused cardiac lipid accumulation in *db/db* mice (Fig. 5B - C). We further examined the lipid levels in the cardiac tissue of the mice in each group, and found that statins treatment mainly caused a significant increase in cardiac FFA and TG levels, while TCHO and LDL-C had no significant difference (Fig. 5D). Most importantly, we found that lipid accumulation was accompanied by aberrant high expression of SREBP1 through Nile red staining and immunofluorescence SREBP1 staining (Supplementary Fig. 5A). On the basis of the aberrantly high expression of SREBP1 in cardiomyocytes of statins-treated *db/db* mouse hearts, we next examined cardiac histology and cardiac systolic function in diabetic *srebp1*-deficient mice and their WT littermates in response to statins treatment. We first tested the genotype of srebp1-deficient mice and the expression of srebp1 in the hearts of diabetic mice to determine that srebp1 is reduced (Supplementary Fig. 6A - C). Indeed, we found that statins therapy had no influence on the ejection fraction or fractional shortening of diabetic *srebp1*-deficient mice compared to the STZ and STZ + ATO10 groups (Fig. 5E, H, I). Consistent with the echocardiographic results, statins therapy had no influence in cardiac fibrosis of diabetic *srebp1*-deficient mice compared to the STZ and STZ + ATO10 groups (Fig. 5F, J). Additionally, we detected the expression of the lipid peroxidation -associated phenotype markers 4-HNE, which confirmed that statins therapy had no influence on cardiac lipid peroxidation in diabetic *srebp1*-deficient mice (Fig. 5G, K). To date, we have shown that cardiac lipid accumulation is associated with aberrant high expression of SREBP1, and genetic knock down of SREBP1 alleviated statins-induced cardiac fibrosis and dysfunction in STZ-induced diabetic mice.

Glucose-mediated glycosylation promotes SREBP-cleavage activating protein (SCAP) trafficking to the Golgi leading to SREBP activation in NMPCs

Up to this point, we next sought to investigate how statins treatment upregulates SREBP expression in cardiomyocytes and is translocated to the nucleus. Previous studies have shown that increasing

intracellular glucose, promotes N-glycosylation of SCAP and consequent activation of SREBP1 in tumorigenesis[22]. To this end, we hypothesized that statins treatment increases the intracellular accumulation of glucose, and the consequent activation of SREBP1. To address this, we conducted PAS staining, and detection of the glucose content indicated massive glycogen deposition in cardiomyocytes of statins-treated *db/db* mice (Fig. 6A, C, E, F). We also observed that, in addition to the heart, glucose uptake and glycogen deposition were similarly increased in the kidneys and muscles of *db/db* mice (Supplementary Fig. 7A - B). We found that statins treatment significantly upregulated the expression of RAGE in cardiomyocytes (Fig. 6B to G, Supplementary Fig. 7C - D). Interestingly, ^{18}F-FDG PET/CT in vivo demonstrated that statins treatment *db/db* mice exhibited no difference in cardiac glucose uptake compared with *db/db* control mice (Fig. 6D, H). Next, we used western blot to detect enzymes of glycolysis in the heart (Fig. 6I to J). We found that the key enzyme, the first step of glycolysis, hexokinase 2 (HK2) did not change significantly, but other downstream metabolic enzymes, such as phosphofructokinase (PFKM), pyruvate kinase M2 (PKM2), and glyceraldehyde-3-phosphate dehydrogenase (GAPDH), significantly decreased in the statin treatment groups. At the same time, glycogen synthase 1 (GYS1) significantly increased, which suggested that statins might reduce glucose utilization, while an increase in the synthesis of glycogen in *db/db* mice (Fig. 6K). This effect was mediated, at least in part, through statins increases IR in *db/db* mice[23]. At the same time, we also detected the AKT-mTOR signaling pathway in the heart, which is related to IR, confirming that statins can activate the AKT-mTOR signaling pathway (Supplementary Fig. 8A - C). Collectively, under the pathological conditions of T2DM, cardiac glucose uptake remains unchanged, but statins treatment can increase cardiac IR, which impairs cardiac glucose utilization, leading to glycogen deposition in diabetic hearts.

To explore the mechanisms by which glucose enhances SCAP protein levels and activates SREBP, NMPCs were cultured in the absence or presence of glucose (25 mmol/L) and atorvastatin for 24 hours, and SREBP1 and SCAP processing was analyzed by immunoblot and immunofluorescence microscopy. Additionally, N-acetylglucosamine (GlcNAc; 20 mmol/l) facilitated N-glycosylation, and tunicamycin (Tuni; 1 mg/ml) was an effective inhibitor of N-glycosylation. The immunoblot data (Fig. 7A - B) showed that GlcNAc enhanced SCAP protein levels and promoted SREBP-1 cleavage; conversely, exposure of cells to Tuni reduced both SCAP protein levels and SREBP-1 cleavage. As expected, exposure of cells to glucose (25 mmol/L) with atorvastatin was as effective as treatment with GlcNAc at enhancing SCAP protein levels and promoting SREBP-1 cleavage, while adding Tuni at the same time inhibited these effects (Fig. 7A - B). In parallel, downstream targets for SREBP1, i.e., fatty acid synthase (FASN), ACC1, stearoyl-coenzyme A desaturase 1 (SCD1), were consistent with SREBP1 (Fig. 7A - B). Immunofluorescence imaging showed that under Tuni exposure conditions, even with supplementation with high glucose and atorvastatin, SREBP1 was still retained in the endoplasmic reticulum (ER) membrane as shown by co-staining with protein disulfide isomerase (PDI), an ER membrane protein. Converse results were observed with GlcNAc or high glucose with atorvastatin treatment (Fig. 7C). SREBP stability, transport to the Golgi and cleavage require the formation of a complex between SREBP and SCAP[22,24]. We observed that GlcNAc or glucose (25 mmol/L) with atorvastatin treatment had the same effect on SCAP and SREBP1

trafficking to the Golgi and subsequent SREBP1 activation, N-terminal fragment of epitope-tagged SREBP in the nuclear as shown by costaining with nuclear DAPI and Golgin, a Golgi protein marker (Fig. 7D - E). Opposite results were observed in the Tuni treatment.

Previous studies have confirmed that SCAP contains a luminal region (a.a. 540–707) with two N-glycosylation sites that are protected from proteolysis when intact membranes are treated with trypsin[25]. This luminal fragment has a molecular weight of approximately 30 kDa and allows the resolution of individual glycosylation variants of SCAP by SDS-PAGE (Fig. 7F). Next, we wondered whether SCAP N-glycosylation is associated with atorvastatin treatment in human AC-16 cardiomyocytes. Within the physiological glucose concentration, N-glycans of SCAP showed that the apparent mass of the fewest trypsin protected fragments decreased (without glycans) after PNGase F digestion (Fig. 7F, Lane 1). Excess glucose and atorvastatin showed that the apparent mass of the most trypsin protected fragments decreased (without glycans) after PNGase F digestion (Fig. 7F, Lane 3). Tuni nearly abolished SCAP N-glycosylation, showing the two weaker bands of the most trypsin protected fragments, even in the presence of high glucose and atorvastatin stimulation. Taken together, these data demonstrate that under high glucose conditions, atorvastatin induced SCAP N-glycosylation and promoted SCAP trafficking to the Golgi, leading to SREBP activation.

Statins therapy combined with L-carnitine alleviates statins-induced cardiac dysfunction and pathological remodeling

We further explored how to alleviate cardiac dysfunction associated with statins therapy in *db/db* mice. Previous studies have shown that L-carnitine treatment enhances FAO and carnitine palmitoyltransferase I (CPTI) expression, furthermore L-carnitine supplementation might be an effective tool for improvement of glucose utilization in T2DM[26], which is important in the pathogenesis of multiple cardiovascular disorders[27]. More importantly, L-carnitine significantly down-regulated the expressions of SREBP1[28]. We found that the content of L-carnitine in the heart tissue of *db/db* mice was significantly lower than that of *db/m* control mice, while there was no significant difference after statins treatment compared with *db/db* control mice (Fig. 8A). We also supplemented *db/db* mice with L-carnitine (300 mg/kg) in the absence or presence of atorvastatin by oral gavage once daily. After supplementation with L-carnitine, we found that the content of L-carnitine in the heart tissue of *db/db* mice was significantly increased (Fig. 8A). At the same time, the ejection fraction and fractional shortening did not decrease significantly after *db/db* mice were supplemented with L-carnitine and atorvastatin (Fig. 8B to C). Histopathologic analysis of the myocardial tissue showed that supplementation with L-carnitine and atorvastatin effectively reduced myocardial injury, cardiac fibrosis and glycogen deposition (Fig. 8D – F, I). Then we detected the expression levels of SREBP1 and 4HNE in the heart. We confirmed that statins combined with L-carnitine could effectively reduce the expression of SREBP1 and alleviate cardiac lipotoxicity ((Fig. 8G – H, J - K). These results indicate that, under the pathological conditions of T2DM, statins therapy combined with L-carnitine may abolish statins-induced cardiac dysfunction and pathological remodeling.

Taken together, our results have shown that long-term statins administration accelerated cardiac endogenous fatty acid synthesis by enhancing the intracellular accumulation of glucose, promoting SCAP N-glycosylation and leading to SREBP-1 activation, which promotes cardiac lipotoxicity and cardiac dysfunction (Supplementary Fig. 9).

Discussion

Over the past few decades, a large body of clinical studies has shown that, even with lipid-lowering drug therapy to a low triglyceride level, and a well-controlled LDL cholesterol level, the incidence of cardiovascular events was not significantly lower in diabetes[8,29–31]. PROMINENT Clinical Trials further highlight the complexity of lipid mediators of residual risk among patients with IR who are receiving statin therapy[8]. Especially under the pathological conditions of T2DM, metabolic maladaptation can occur and there is a great loss of metabolic flexibility due to IR, leading to intramyocardial lipid accumulation[23]. Metabolic abnormalities in the diabetic heart may impair the cardioprotective effect of statins in T2DM patients. Thus, to improve the cardiovascular benefit of statins in people with T2DM, it is necessary to eliminate the detrimental effects statins on cardiac metabolic homeostasis. In this study, we have suggested 3 major findings. First, our findings reveal a novel viewpoint, reducing blood lipids is not equivalent to lowering lipids in the heart. Second, long-term statins administration worsens diabetes-induced cardiac dysfunction in diabetic mice. Thirdly, the underlying mechanism is lipid accumulation caused by abnormal activation of endogenous FA synthesis through the SREBP1 lipogenesis pathway in cardiomyocytes.

Guidelines recommend statins therapy for all T2DM patients who are 40 to 75 years old and have an LDL-C level of 70 mg/dL or greater for primary prevention of CVDs[32]. Previous studies have shown patients treated with statin therapy had increased IR, hemoglobin A1c (HbA1c) levels, and fasting plasma glucose levels[33,34]. Importantly, progression of IR is of concern because it may lead to metabolic syndrome exacerbating diabetes disease progression. It is important to understand the link between increased IR and cardiovascular complications in T2DM. A retrospective matched-cohort study showed that statins therapy was associated with diabetes progression in diabetes, and statin users had a higher likelihood of developing significant hyperglycemia, experiencing acute glycemic complications[35]. In our study, we also retrospectively analyzed the clinical characteristics of diabetic patients treated with statins, and we obtained the same results. Statins significantly aggravated IR in diabetic patients, furthermore hs-TnT and CK increased significantly. In general, insulin signaling regulates glucose and lipid metabolism in the heart, maintaining cardiometabolic homeostasis. However, IR produces metabolic derangements leading to increased lipid oxidation and decreased glucose oxidation[23]. Despite major recognition of statins-elicited metabolic and IR adverse effects, few studies have compared the time effects of statins-induced metabolic and cardiac outcomes in diabetes.

Using three types of diabetic mice and a clinically comparable dose of statins, within 40 weeks of consecutive treatments, we observed that statins therapy worsened diabetes-induced cardiac dysfunction

and pathological remodeling compared with *db/db* mouse controls. From the results of echocardiography and single-cell contraction assays, in the statins-treated group, cardiac contractile and relaxation functions were impaired, and ventricular conduction velocity was slowed. In addition, histopathologic analysis of myocardial tissue revealed that statins treatment in *db/db* mice significantly promoted cardiac interstitial fibrosis, inflammatory infiltrates, and cardiomyocyte myofibrillar arrangement. While different mechanisms can induce changes of cardial structure and cardiac function, metabolic dysfunction may predominate in inducing cardiac dysfunction. The general concept is that free fat acids (FFAs) are the major substrate for ATP production in adult cardiac mitochondria, providing 60 and 70% of the energy of the heart[23]. When diabetes progresses or IR increases, the cardiomyocytes decrease their ability to use fatty acids, increasing FFAs delivery and leading to intramyocardial lipid accumulation[36]. This intramyocardial lipid accumulation may lead to mitochondrial dysfunction in cardiomyocytes. Furthermore, mitochondrial dysfunction is associated with increased ROS production, leading to increased oxidative damage, and reduced ATP production, which includes sulfhydryl oxidation, lipid peroxidation, and mitochondrial DNA mutation[37]. Mitochondrial dysfunction is particularly important in directing cardiomyocytes injury. Our electron microscopy results of myocardial tissue suggested that the mitochondria of statins-treated *db/db* mice exhibited swelling and cristolysis, that is, the lysis and breakdown of mitochondrial cristae. Interestingly, we observed mitochondrial dysfunction in cardiomyocytes accompanied by massive lipid droplet deposition by electron microscopy and oil red O staining. Given the increased mitochondrial dysfunction and lipid droplet deposition observed in statins-treated *db/db* mouse hearts, we hypothesized that abnormal lipid metabolism leads to massive lipid deposition causing mitochondrial dysfunction, thereby accelerating cardiomyocyte dysfunction.

Lipid metabolism involves multiple biological processes involved in the synthesis or utilization of lipids. Interestingly, we observed potent expression of the SREBP1 lipogenesis pathway in statins-treated *db/db* mouse hearts. We further confirmed that SREBP1-N was significantly upregulated and translocated to the nucleus in the myocardium of statins-treated *db/db* mice. SREBP1 downstream targeting enzymes such as FASN, ACC1, and SCD1 were synchronously upregulated. Most importantly, we found that lipid accumulation was accompanied by aberrantly high expression of SREBP1 in cardiomyocytes. In general, the general concept that the heart can only utilize but not synthesize lipids. However, that may not be the case. As early as the 1860s, W. C. HÜLSMANN et al. and other scholars confirmed that the myocardium has a marginal capacity for de novo lipogenesis and is stimulated by succinate, a uniquely potent stimulant. The rate of synthesis is mediated by alterations in the NADH: NAD^+ ratio and this ratio is an effective regulator of the system[38,39]. Under special conditions, such as fasting or diabetes, the heart can initiate fatty acid synthesis in the mitochondrial system[40]. The failure of glycogen utilization during fasting and diabetes might be associated with the heart's unaltered lipogenetic activity. Next, we verified whether cardiomyocytes could synthesize fatty acids and whether statin stimulation increased fatty acid synthesis in vitro. We traced the metabolic fluxes in statins induced NMPCs and observed generally increased intermediates in fatty acid de novo synthesis pathways, further confirming that statins treatment promotes increased de novo synthesis of lipids in cardiomyocytes under high glucose conditions.

SREBPs, including SREBP-1a, SREBP-1c, and SREBP-2, are transcription factors involved in the regulation of lipid homeostasis, and are responsible for the transcriptional activation of genes associated with the synthesis of triglycerides, fatty acids, and cholesterol[41]. In earlier studies, SREBP1 activation was shown to induce lipid accumulation and lipotoxicity in diabetic kidneys[42]. Under basal physiological conditions, the C-terminal domain of SREBP1 binds to SCAP in the ER membrane. When cells are deprived of cholesterol and high cellular glucose[22], SCAP is recognized by cytoplasmic coat protein complex II (COPII) and escorts SREBP1 to the Golgi, where it is subsequently cleaved by site-1 protease (S1P) and site-2 protease (S2P). Finally, the N-terminal transcription factor domain of SREBPs is released for nuclear translocation. This nuclear form of SREBP1 (nSREBP1) binds the sterol regulatory element (SRE) and then activates target gene expression. In contrast, when cholesterol accumulates in the ER, the SCAP-SREBP complex is retained in the ER by binding to insulin-induced gene (INSIG), and thus the activation of SREBP is blocked[43]. Previous studies have revealed that[22] there are three N-glycosylation sites on SCAP that enhance SCAP N-glycosylation and its protein levels leading to the movement of SCAP/SREBP to the Golgi and consequent proteolytic activation of SREBP1. Similar phenomena of increased lipogenesis and activated SREBP-2 are observed in hyperphosphatemic chronic kidney disease (CKD) mouse models[44]. Here we tested the hypothesis that statins lead to increased intracellular glucose in cardiomyocytes, thereby enhancing SCAP N-glycosylation and its protein levels, and consequent proteolytic activation of SREBP1. We found that in the presence of high glucose, which simulates the cellular state of diabetes, statins could enhance SCAP N-glycosylation and propel SCAP/SREBP trafficking and subsequent SREBP1 activation. We further verified in the human heart that in the state of diabetes, cardiomyocytes highly express SREBP1, which is associated with cardiac fibrosis and lipid peroxidation. Clearly, our mechanistic studies still leave much to be desired. For example, we need to further verify the glycosylation site on SCAP and identify the binding motif for insig or SCAP for N-linked oligosaccharide.

Finally, we proposed L-carnitine, enhanced FAO and glucose utilization as an effective means of rescuing intramyocardial lipid accumulation induced by statins. We found that statins therapy combined with L-carnitine may abolish statins-induced cardiac dysfunction and pathological remodeling. This means that combined drugs targeting lipid and glucose metabolism may be a potential target to address the metabolic effects by patients on lipid-lowering drug therapy, which may effectively reduce the risk of cardiovascular events.

In conclusion, our data are in agreement with Prof. Ishak A Mansi's view[35], and we need to highlight that statins therapy was associated with diabetes progression, including significant hyperglycemia and increased IR, especially cardiovascular complications. This suggests that clinicians should take into consideration the metabolic effects and risk-benefit ratio when prescribing statins therapy in diabetic patients. Furthermore, our findings reveal a novel viewpoint, reducing blood lipids is not equivalent to lowering lipids in the heart, which should be considered in lipid-lowering therapy to better reduce cardiovascular risk. This effect may also contribute to the design of effective dual therapeutic strategies

targeting both hyperlipidemia and IR in the T2DM population. Targeting SREBP-1-mediated lipogenesis as potential strategies for lowering lipids in the heart.

A limitation of this current study is the lack of clinical data of long-term statins treatment for T2DM patients. In particular the mechanistic insight into the glucose accumulation resulting in SREBP1 induction or whether N-glycans of SCAP inhibition can prevent statins treatment induce diabetes cardiac dysfunction. Most importantly, future studies need to investigate that cardiomyocyte can synthesize FAs under specific pathological conditions in vivo.

Methods

Ethics statement

All experiments performed in this study were compiled with ethical regulations and approved by the Animal Care and Ethics Committee of Sun Yat-sen University. The details are described in the respective sections below.

A cross-sectional study in Chinese diabetes population

We conducted a cross-sectional study to investigate the outcomes of diabetic patient's statins administration. All hospitalized patients diagnosed with T2DM in the department of endocrinology, Sun Yat-sen Memorial Hospital from January 2019 to October 2022 were retrospectively reviewed: group A (Non-statins user), a total of 291 patients who treated without atorvastatin; group B (statins user), a total of 108 patients who treated with atorvastatin. Patients who met the following criteria were excluded: acute myocardial infarction, stroke, cancer, severe cardiomyopathy etc. All medical test results of patients are collected by the hospital's medical records system. The data in this study will be used only for research statistical purposes and in ways that will not reveal the patient's private information. The Sun Yat-sen Memorial Hospital ethic committee approved this study (grant No.: SYSKY-2022-015-01) and waived the need for patients' consent. These patients' right of privacy has been well protected in clinical diagnosis and treatment. The study was conducted in accordance with the Declaration of Helsinki (2013).

Human subjects

Heart samples from 10 healthy populations and 12 T2DM patients used in this study were collected from the National Center for Medico-legal Expertise of Sun Yat-sen University. The use of human heart samples was approved by the ethics committee of Zhongshan School of Medicine, Sun Yat-sen University (grant No.: 2019-004) and all data and sample collection were in strict accordance with ethics guidelines of Zhongshan School of Medicine, Sun Yat-sen University. Informed consent was obtained from the legal representatives of the victims. The principles outlined in the Declaration of Helsinki were followed. Please refer to Supplementary Table 2 for information about the decedents' age, sex, and heart details.

Animal Experiments

Four-week-old male C57BLKS/J$^{db/db}$ (*db/db*) mice, age-matched male non-diabetic C57BLKS/J$^{db/m}$ (*db/m*) mice were purchased from GemPharmatech Co., Ltd (Jiangsu, China) following breeding at the Center for Disease Model Animals of Sun Yat-sen University. Ten-weeks-old male *db/db* mice and *db/m* mice were enrolled in these experiments and divided into five groups: Db/m group, Db group, Db + Ato5 group (atorvastatin 5 mg.kg^{-1} BW/day), Db + Ato10 group (atorvastatin10 mg.kg^{-1} BW/day) and Db + Rosu20 group (Rosuvastatin 20 mg.kg^{-1} BW/day). In addition, we also used *db/m* mice as a control group administered statins and divided into four groups: Db/m + Ato5 group, Db/m + Ato10 group; Db/m + Rosu20 group. The drugs were dissolved in saline and administered through oral gavage once a day for 40 weeks. All animals were given water and chow diet during the whole experiment period. During this period, body weight, fasting blood glucose (FBG) were measured.

The experimental grouping, and statins treatment of streptozotocin (STZ)-induced T2DM mouse model and KK-Ay diabetic mice were the same as those of *db/db* mice. All animal experiments details were described previously in our paper[11].

SREBP1-KO mice (Strain NO. T037279, genetic background: C57BL/6J) were purchased from GemPharmatech (Nanjing, China). Heterozygous F0 generation mice were obtained by freezing sperm resuscitation. After hybridization of F0 generation mice, F1 generation heterozygous mice (SREBP1$^{+/-}$) were obtained for STZ induce T2DM model (8 weeks old). The experimental grouping, and statins treatment were the same as those of *db/db* mice.

All mice were housed in an animal facility with a 12 hours light–dark cycle and water. All animal experiments were performed according to the regulations approved by the Animal Care and Ethics Committee of Sun Yat-sen University (the protocol number is 2021000957).

Cardiomyocyte contractility assay

Following existing literature methods[45,46], we used the integrated IonOptix contractility/ photometry system to measure sarcomere shortening and relaxation in freshly isolated left ventricular cardiomyocytes from mouse hearts. Cardiomyocytes were maintained in normal Tyrode solution after being restored to calcium ion concentration at room temperature. An electric field of 1 Hz was set with a myopacer (IonOptix MYP100) through platinum electrodes lowered into the bath for electrical stimulation of cardiomyocytes while tracking sarcomere transient traces and sarcomere length changes. Basal and peak sarcomere lengths, maximum departure and return velocities, and time to peak or to baseline were measured. All measurements were performed at room temperature within 3 h. Data were collected and analyzed using IonWizard 7.4.

Assessment of indirect calorimetry

Indirect calorimetry data were recorded in the studied mice by using a Promethion Metabolic Cage System (Sable Systems, USA) as described previously[47]. Mice were acclimated for 2 days in metabolic cages before recording calorimetric variables. Animals were housed individually in metabolic chambers

maintained at 28°C under a 12 hours light/dark cycle with free access to food and water. Oxygen consumption (VO_2) and carbon dioxide production (VCO_2) for individual mice were measured. The respiratory exchange ratio (RER) was calculated as VCO_2/VO_2. Other indicators calculated as described previously[47].

Transmission electron microscopy (TEM).

Cardiac ultrastructure was examined under a transmission electron microscope (Tecnai G2 SpiritTwin + GATAN 832.10W, FEI, Czech) using conventional methods. In brief, heart tissues were fixed with 2.5% glutaraldehyde in 0.1 mol/L phosphate buffer (pH 7.4), followed by 1% OsO4. After dehydration, thin sections were stained with uranyl acetate and lead citrate for observation, images were acquired digitally.

Terminal deoxynucleotidyl transferase-mediated dUTP nick end labeling (TUNEL) staining.

TUNEL staining was performed using the Colorimetric TUNEL Apoptosis Assay Kit (Beyotime, Shanghai, China). The positive cell numbers were counted from several fields per sample with the ImageJ software program (National Institutes of Health, Bethesda, MD, USA).

Histological analysis, WGA-FITC staining and Oil red O staining

The hearts were harvested and fixed overnight in 4% paraformaldehyde and dehydrated with alcohol for paraffin embedding. Heart sections (4 μm) were stained with H&E, Masson's trichrome, Sirius red, Periodic Acid-Schiff (PAS) stain according to standard protocols. All the histological staining images were captured by a microscope (DFC700T, Leica, Germany).

For WGA-FITC staining, the heart sections were incubated with WGA-FITC (Sigma-Aldrich, St. Louis, MO) at 37°C for 30min. All the immune-fluorescence images were captured by a fluorescence microscope (DFC700T, Leica, Germany). The cardiomyocyte area was calculated from several fields per sample with the ImageJ software program (National Institutes of Health, Bethesda, MD, USA).

For Oil red O staining, the heart tissues were fixed in 4% paraformaldehyde (Biosharp, Hefei, China) overnight then dehydrated with a sucrose gradient, and embedded in the Tissue-Tek OCT compound (Sakura Finetek, Tokyo, Japan). Then, the sections (7 μm) were stained with oil red O (G1261, Beijing Solarbio Science & Technology Co., Ltd., Beijing, China) for 20 minutes.

Immunohistochemistry (IHC) and Immunofluorescence (IF)

The heart samples sections were blocked with 3% hydrogen peroxide and then performed at 95°C for 10min using citrate buffer (Beyotime, Shanghai, China), then blocking steps were carried out using the QuickBlock™ Blocking Buffer (Beyotime, Shanghai, China) according to the manufacturer's instructions. The sections were then incubated with antibodies. After incubated with primary antibody at 4°C overnight, the sections incubated with secondary antibody (Beyotime, Shanghai, China) at 37°C for 30min.

Visualization was accomplished using 3,3N-diaminobenzidine tertrahydrochloride (DAB) (Beyotime, Shanghai, China). Sections were counterstained with hematoxylin (Solarbio, Beijing, China). In the negative controls, the primary antibody was omitted and replaced with the blocking solution. All the histological staining and immune-fluorescence images were captured by a microscope (DFC700T, Leica, Germany). The positive area was quantified with the ImageJ software program (National Institutes of Health, Bethesda, MD, USA). The antibodies are listed in Supplementary Table 3.

Immunoblot analysis

For western blotting analysis, an equal number of proteins (30 mg) was resolved by an 8–12% gel, transferred to polyvinylidene fluoride (PVDF) membranes (Millipore, Burlington, MA, USA), and incubated with appropriate primary antibodies at 4°C overnight. Membranes were washed three times by Tris-buffered saline containing 0.1% tween-80 (TBST) and incubated with peroxidase-conjugated secondary antibodies. Protein bands were visualized with the enhanced chemiluminescence (ECL) reagent using a ChemiDoc MP Imaging System (Bio-Rad Co., Hercules, CA, USA). The antibodies are listed in Supplementary Table 3.

Serum/ tissue measurement

The serum brain natriuretic peptide (BNP) levels were examined using an enzyme-linked immunosorbent assay (ELISA) (CSB-E07971m, Cusabio, Wuhan, China). The heart tissue TG, TCHO, LDL and HDL levels were examined using commercial reagent kits (Jiancheng, Nanjing, Jiangsu, China). The heart and liver tissue glucose levels were examined using commercial reagent kits (ADS078TC0, Jiangsu Meimian Industrial Co., Ltd, Jiangsu, China)

Vitro experiment groups for western blot analysis and IF

NMPCs were subjected to starvation in a serum-free medium overnight, then divide into 6 groups, respectively cultured in glucose 1.0 mmol/L (group 1), cultured in a glucose 4.5 mmol/L (group 2), the group 3 treated with glucose 4.5 mmol/l and atorvastatin 10 μmol/L (Sigma-Aldrich, PHR1422), the group 4 treated with tunicamycin (1 μg/mL) (ab120296, Abcam), the group 5 treated with GlcNAc (20 mM) (S6257, Selleck Chemicals), the group 6 treated with glucose 4.5 mmol/L and atorvastatin10 mmol/l, tunicamycin (1 μg/mL). All groups NMPCs were cultured for 24 hours. The experiment was repeated three times.

Detection of SCAP N-glycosylation

The human AC-16 cardiomyocytes were subjected to starvation in a serum-free medium overnight, then divide into 6 groups, respectively cultured in glucose 1.0 mmol/L (group 1), cultured in a glucose 4.5 mmol/L (group 2), the group 3 treated with glucose 4.5 mmol/L and atorvastatin 10 μmol/L, the group 4 and 5 treated with tunicamycin (1 μg/mL), the group 6 and 7 treated with glucose 4.5 mmol/l and atorvastatin 10 μmol/L and tunicamycin. All groups AC-16 cardiomyocytes were cultured for 24 hours. And then detection of SCAP N-glycosylation. The groups of 1, 2, 3, 5, and 7 subsequent treatments with PNGase F. The experiment was repeated three times.

The detection of SCAP N-glycosylation was performed according to the method described previously[22,48]. Briefly, the membrane pellets from cell lysates prepared as described above were resuspended in 114 μL of buffer containing 10 mM HEPES·KOH (pH 7.4), 10 mM KCl, 1.5 mM $MgCl_2$, 1 mM sodium EDTA, and 100 mM NaCl. Aliquots of membrane proteins were then incubated in the absence or presence of 1 μg of trypsin (T6567, Sigma), in a total volume of 58 μL, for 30 min at 30°C. Reactions were stopped by the addition of 2 μL (400 units) of soybean trypsin inhibitor (T9777, Sigma). The samples were then heated at 100°C for 10 min with 5x loading buffer and subjected to SDS-PAGE. Combine 1–20 μg of glycoprotein, 1 μL of Glycoprotein Denaturing Buffer (10X) and H2O (if necessary) to make a 10 μL total reaction volume. Denature glycoprotein by heating reaction at 100°C for 10 minutes. Chill denatured glycoprotein on ice and centrifuge 10 seconds. Make a total reaction volume of 20(40) μL by adding 2 μL GlycoBuffer 2 (10X), 2 μL 10% NP-40 and 6 μL H2O. Add 1 μL PNGase F, mix gently. Incubate reaction at 37°C for 1 hour. The mixtures were heated at 100°C for 10 min and subjected to SDS-PAGE.

Statistical Analysis

All statistical analysis was performed using Prism 9 (GraphPad Software Inc) and IBM SPSS Statistics software (SPSS) (Versions 22.0) (Inc., Chicago, IL). Data are expressed as mean ± SEM. All experiments were repeated at least 3 times with representative data shown. A two-tailed unpaired Student t-test was performed to determine the difference between 2 groups. For comparisons of ≥ 3 groups, two-tailed, One-way ANOVA followed by Tukey's test was performed. For correlation analysis, linear regression models were performed and the goodness of fit for regression models was assessed using R values. All group

numbers and detailed significant values were presented within the figure or their legends. *P* values < 0.05 were considered to indicate statistically significant differences.

Declarations

Data Availability Statement

Source data contained the raw data underlying the following types of display items: any reported means/averages in bar charts, and tables, and uncropped versions of any gels or blots, labelled with the relevant panel and identifying information. Source data are provided with this paper.

Acknowledgments

T.H., T.W. contributed equally to this work. The authors sincerely thank Prof. Jianding Cheng (Department of Forensic Pathology, Zhongshan School of Medicine, Sun Yat-sen University) for providing human heart samples for this study. The authors acknowledge Dr. Tiantian Yu (Metabolic Innovation Center, Sun Yat-Sen University) for her help in metabolic flux analysis. W.C. is supported by National Key Research and Development Program of China (Grant No.2019YFA0801403), National Nature Science Foundation of China (Grant No. 82370283, 82170261, 81970219), Guangdong Basic and Applied Basic Research Foundation (Grant Number: 2021A1515011005, 2021A1515110233 and 2021B1212040006), Guangzhou

Municipal Science and Technology Bureau (Grant Number: 2019030015). J.T. is supported by National Nature Science Foundation of China (Grant Number:82200289) and Guangdong Basic and Applied Basic Research Foundation (Grant Number: 2021A1515110233). The funders had no role in study design, data collection and analysis, decision to publish, or preparation of the manuscript.

Conflict of Interest

The authors declare no conflict of interest.

Data Availability Statement

The data that support the findings of this study are available from the corresponding author upon reasonable request.

References

1. Arnold SV et al (2021) Type 2 diabetes and heart failure: insights from the global DISCOVER study. ESC Heart Fail 8:1711–1716. 10.1002/ehf2.13235
2. Gregg EW et al (2012) Trends in death rates among U.S. adults with and without diabetes between 1997 and 2006: findings from the National Health Interview Survey. Diabetes Care 35:1252–1257. 10.2337/dc11-1162
3. Trialists CT (2008) Efficacy of cholesterol-lowering therapy in 18,686 people with diabetes in 14 randomised trials of statins: a meta-analysis. Lancet 371:117–125. 10.1016/S0140-6736(08)60104-X
4. Arnett DK et al (2019) ACC/AHA Guideline on the Primary Prevention of Cardiovascular Disease: A Report of the American College of Cardiology/American Heart Association Task Force on Clinical Practice Guidelines. *Circulation* 140, e596-e646, 10.1161/CIR.0000000000000678 (2019)
5. Colhoun HM et al (2004) Primary prevention of cardiovascular disease with atorvastatin in type 2 diabetes in the Collaborative Atorvastatin Diabetes Study (CARDS): multicentre randomised placebo-controlled trial. Lancet 364:685–696. 10.1016/S0140-6736(04)16895-5
6. Sever PS et al (2005) Reduction in cardiovascular events with atorvastatin in 2,532 patients with type 2 diabetes: Anglo-Scandinavian Cardiac Outcomes Trial–lipid-lowering arm (ASCOT-LLA). Diabetes Care 28:1151–1157. 10.2337/diacare.28.5.1151
7. Knopp RH, d'Emden M, Smilde JG, Pocock SJ (2006) Efficacy and safety of atorvastatin in the prevention of cardiovascular end points in subjects with type 2 diabetes: the Atorvastatin Study for Prevention of Coronary Heart Disease Endpoints in non-insulin-dependent diabetes mellitus (ASPEN). Diabetes Care 29:1478–1485. 10.2337/dc05-2415
8. Das Pradhan A et al (2022) Triglyceride Lowering with Pemafibrate to Reduce Cardiovascular Risk. N Engl J Med 387:1923–1934. 10.1056/NEJMoa2210645

9. Group AS et al (2010) Effects of combination lipid therapy in type 2 diabetes mellitus. N Engl J Med 362:1563–1574. 10.1056/NEJMoa1001282
10. Da Dalt L et al (2021) PCSK9 deficiency rewires heart metabolism and drives heart failure with preserved ejection fraction. Eur Heart J 42:3078–3090. 10.1093/eurheartj/ehab431
11. Huang TS et al (2023) Long-term statins administration exacerbates diabetic nephropathy via ectopic fat deposition in diabetic mice. Nat Commun 14:390. 10.1038/s41467-023-35944-z
12. Wu Y et al (2023) Retinol dehydrogenase 10 reduction mediated retinol metabolism disorder promotes diabetic cardiomyopathy in male mice. Nat Commun 14:1181. 10.1038/s41467-023-36837-x
13. Ayyappan JP, Lizardo K, Wang S, Yurkow E, Nagajyothi JF (2020) Inhibition of SREBP Improves Cardiac Lipidopathy, Improves Endoplasmic Reticulum Stress, and Modulates Chronic Chagas Cardiomyopathy. J Am Heart Association 9:e014255. 10.1161/jaha.119.014255
14. Castiglione V et al (2022) Biomarkers for the diagnosis and management of heart failure. Heart Fail Rev 27:625–643. 10.1007/s10741-021-10105-w
15. Vieira AC et al (2016) Heart Alterations after Domoic Acid Administration in Rats. Toxins (Basel) 8. 10.3390/toxins8030068
16. Erlandson KM, Jiang Y, Debanne SM, McComsey GA (2015) Rosuvastatin Worsens Insulin Resistance in HIV-Infected Adults on Antiretroviral Therapy. Clin Infect Dis 61:1566–1572. 10.1093/cid/civ554
17. Koh KK et al (2010) Atorvastatin causes insulin resistance and increases ambient glycemia in hypercholesterolemic patients. J Am Coll Cardiol 55:1209–1216. 10.1016/j.jacc.2009.10.053
18. Henriksbo BD et al (2014) Fluvastatin causes NLRP3 inflammasome-mediated adipose insulin resistance. Diabetes 63:3742–3747. 10.2337/db13-1398
19. Brewster LM et al (2006) Creatine kinase activity is associated with blood pressure. Circulation 114:2034–2039. 10.1161/CIRCULATIONAHA.105.584490
20. McEvoy JW et al (2016) Six-Year Change in High-Sensitivity Cardiac Troponin T and Risk of Subsequent Coronary Heart Disease, Heart Failure, and Death. JAMA Cardiol 1:519–528. 10.1001/jamacardio.2016.0765
21. Shimano H, Sato R (2017) SREBP-regulated lipid metabolism: convergent physiology - divergent pathophysiology. Nat Rev Endocrinol 13:710–730. 10.1038/nrendo.2017.91
22. Cheng C et al (2015) Glucose-Mediated N-glycosylation of SCAP Is Essential for SREBP-1 Activation and Tumor Growth. Cancer Cell 28:569–581. 10.1016/j.ccell.2015.09.021
23. Ormazabal V et al (2018) Association between insulin resistance and the development of cardiovascular disease. Cardiovasc Diabetol 17. 10.1186/s12933-018-0762-4
24. Nohturfft A, Yabe D, Goldstein JL, Brown MS, Espenshade PJ (2000) Regulated step in cholesterol feedback localized to budding of SCAP from ER membranes. Cell 102:315–323. 10.1016/s0092-8674(00)00037-4

25. Nohturfft A, Brown MS, Goldstein JL (1998) Topology of SREBP cleavage-activating protein, a polytopic membrane protein with a sterol-sensing domain. J Biol Chem 273:17243–17250. 10.1074/jbc.273.27.17243
26. Bene J, Hadzsiev K, Melegh B (2018) Role of carnitine and its derivatives in the development and management of type 2 diabetes. Nutr Diabetes 8:8. 10.1038/s41387-018-0017-1
27. Wang M et al (2021) Carnitine Palmitoyltransferase System: A New Target for Anti-Inflammatory and Anticancer Therapy? Front Pharmacol 12:760581. 10.3389/fphar.2021.760581
28. Wang S et al (2023) Dietary L-carnitine supplementation changes lipid metabolism and glucose utilization of Rhynchocypris lagowskii fed diets with different lipid sources. Fish Physiol Biochem. 10.1007/s10695-022-01166-1
29. Nicholls SJ et al (2020) Effect of High-Dose Omega-3 Fatty Acids vs Corn Oil on Major Adverse Cardiovascular Events in Patients at High Cardiovascular Risk: The STRENGTH Randomized Clinical Trial. JAMA 324:2268–2280. 10.1001/jama.2020.22258
30. Investigators A-H et al (2011) Niacin in patients with low HDL cholesterol levels receiving intensive statin therapy. N Engl J Med 365:2255–2267. 10.1056/NEJMoa1107579
31. Itoh H et al (2018) Intensive Treat-to-Target Statin Therapy in High-Risk Japanese Patients With Hypercholesterolemia and Diabetic Retinopathy: Report of a Randomized Study. Diabetes Care 41:1275–1284. 10.2337/dc17-2224
32. American Diabetes A (2018) 9. Cardiovascular Disease and Risk Management: Standards of Medical Care in Diabetes-2018. *Diabetes Care* 41, S86-S104, 10.2337/dc18-S009
33. Liew SM et al (2014) Statins use is associated with poorer glycaemic control in a cohort of hypertensive patients with diabetes and without diabetes. Diabetol Metab Syndr 6:53. 10.1186/1758-5996-6-53
34. Cederberg H et al (2015) Increased risk of diabetes with statin treatment is associated with impaired insulin sensitivity and insulin secretion: a 6 year follow-up study of the METSIM cohort. Diabetologia 58:1109–1117. 10.1007/s00125-015-3528-5
35. Mansi IA et al (2021) Association of Statin Therapy Initiation With Diabetes Progression: A Retrospective Matched-Cohort Study. JAMA Intern Med 181:1562–1574. 10.1001/jamainternmed.2021.5714
36. D'Souza K, Nzirorera C, Kienesberger PC (2016) Lipid metabolism and signaling in cardiac lipotoxicity. Biochim Biophys Acta 1861:1513–1524. 10.1016/j.bbalip.2016.02.016
37. Chen MS, Lee RT, Garbern JC (2022) Senescence mechanisms and targets in the heart. Cardiovasc Res 118:1173–1187. 10.1093/cvr/cvab161
38. Whereat AF, Hull FE, Orishimo MW (1967) The role of succinate in the regulation of fatty acid synthesis by heart mitochondria. J Biol Chem 242:4013–4022
39. Hulsmann WC (1962) Fatty acid synthesis in heart sarcosomes. Biochim Biophys Acta 58:417–429. 10.1016/0006-3002(62)90052-5

40. Whereat AF, Orishimo MW (1969) Effects of fasting and diabetes on fatty acid synthesis by heart mitochondria. Am J Physiol 217:998–1003. 10.1152/ajplegacy.1969.217.4.998
41. Horton JD, Goldstein JL, Brown MS (2002) SREBPs: activators of the complete program of cholesterol and fatty acid synthesis in the liver. J Clin Invest 109:1125–1131. 10.1172/JCI15593
42. Sun L, Halaihel N, Zhang W, Rogers T, Levi M (2002) Role of sterol regulatory element-binding protein 1 in regulation of renal lipid metabolism and glomerulosclerosis in diabetes mellitus. J Biol Chem 277:18919–18927. 10.1074/jbc.M110650200
43. Jiang SY et al (2022) Discovery of an insulin-induced gene binding compound that ameliorates nonalcoholic steatohepatitis by inhibiting sterol regulatory element-binding protein-mediated lipogenesis. Hepatology 76:1466–1481. 10.1002/hep.32381
44. Zhou C et al (2021) Hyperphosphatemia in chronic kidney disease exacerbates atherosclerosis via a mannosidases-mediated complex-type conversion of SCAP N-glycans. Kidney Int 99:1342–1353. 10.1016/j.kint.2021.01.016
45. Chen CY et al (2018) Suppression of detyrosinated microtubules improves cardiomyocyte function in human heart failure. Nat Med 24:1225–1233. 10.1038/s41591-018-0046-2
46. Yu X et al (2021) MARK4 controls ischaemic heart failure through microtubule detyrosination. Nature 594:560–565. 10.1038/s41586-021-03573-5
47. Vu JP et al (2017) Long-Term Intake of a High-Protein Diet Affects Body Phenotype, Metabolism, and Plasma Hormones in Mice. J Nutr 147:2243–2251. 10.3945/jn.117.257873
48. Cheng C et al (2016) Analysis of SCAP N-glycosylation and Trafficking in Human Cells. J Vis Exp. 10.3791/54709

Figures

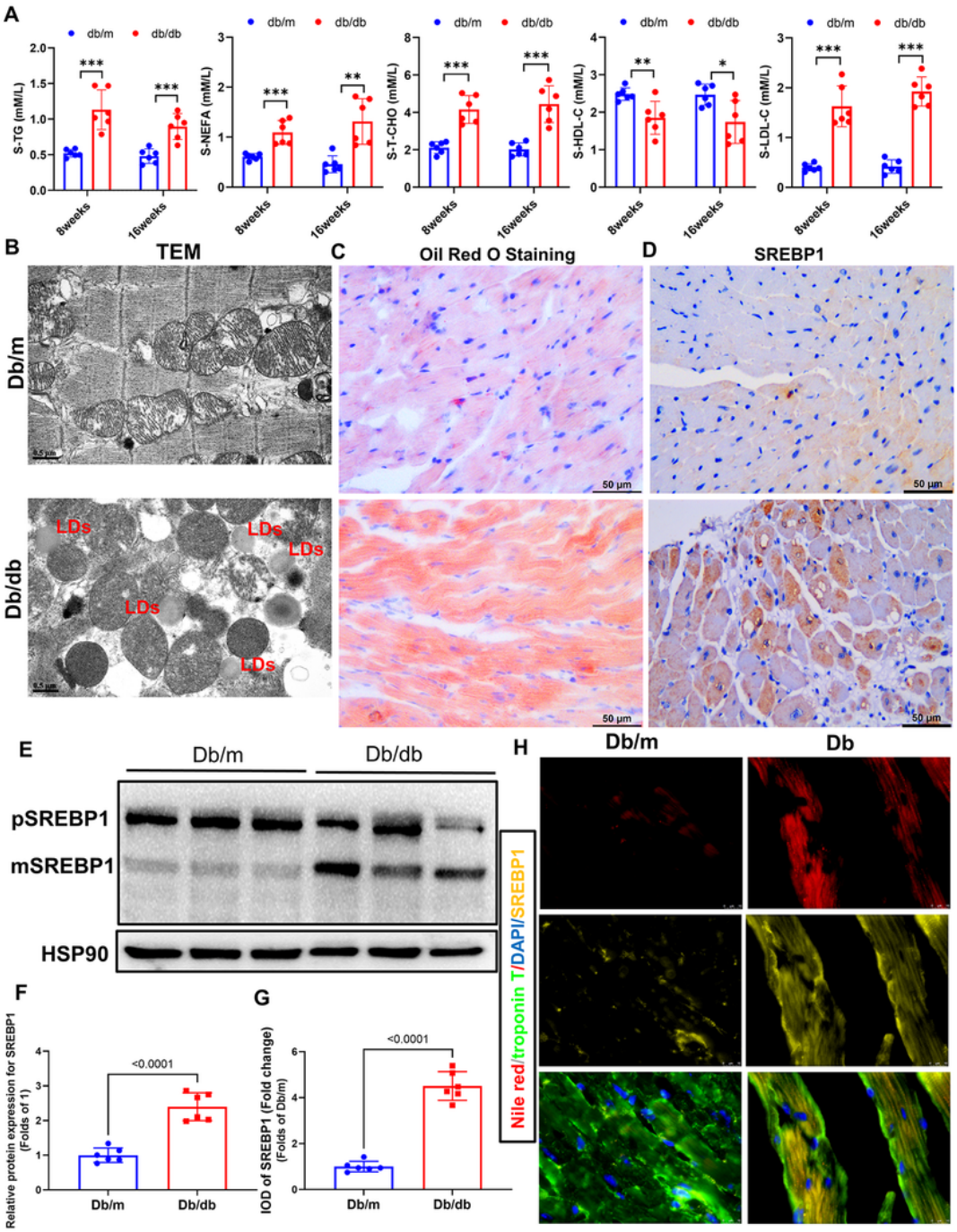

Figure 1

SREBP1 is significantly up-regulated in diabetic myocardium and may be associated lipid accumulation. **(A)**Lipid profile in *db/db* mice. n = 6 in each group. Data are expressed as means ± SEM. **(B)** Representative TEM images in the myocardium. Original magnification ×26500, scale bar = 0.5 μm.**(C)** Representative Oil-red O staining images in the myocardium. **(D)** Immunohistochemistry staining of SREBP1 of heart from each group. Original magnification × 400, scale bar = 50 μm (C-D). **(E-**

F)Representative immunoblot images and quantification of SREBP1. **(G)** Analysis of SREBP1 protein expression in the myocardium according to immunohistochemical staining. n = 6 in each group. Data are expressed as means ± SEM. Student's t test (t test) was used for the analysis of statistical significance. **(H)** Immunofluorescence staining of protein SREBP1 (yellow), Nile red (red) and cardiomyocyte marker Troponin T (green) in the myocardium. Original magnification × 1000, scale bar = 20 μm.

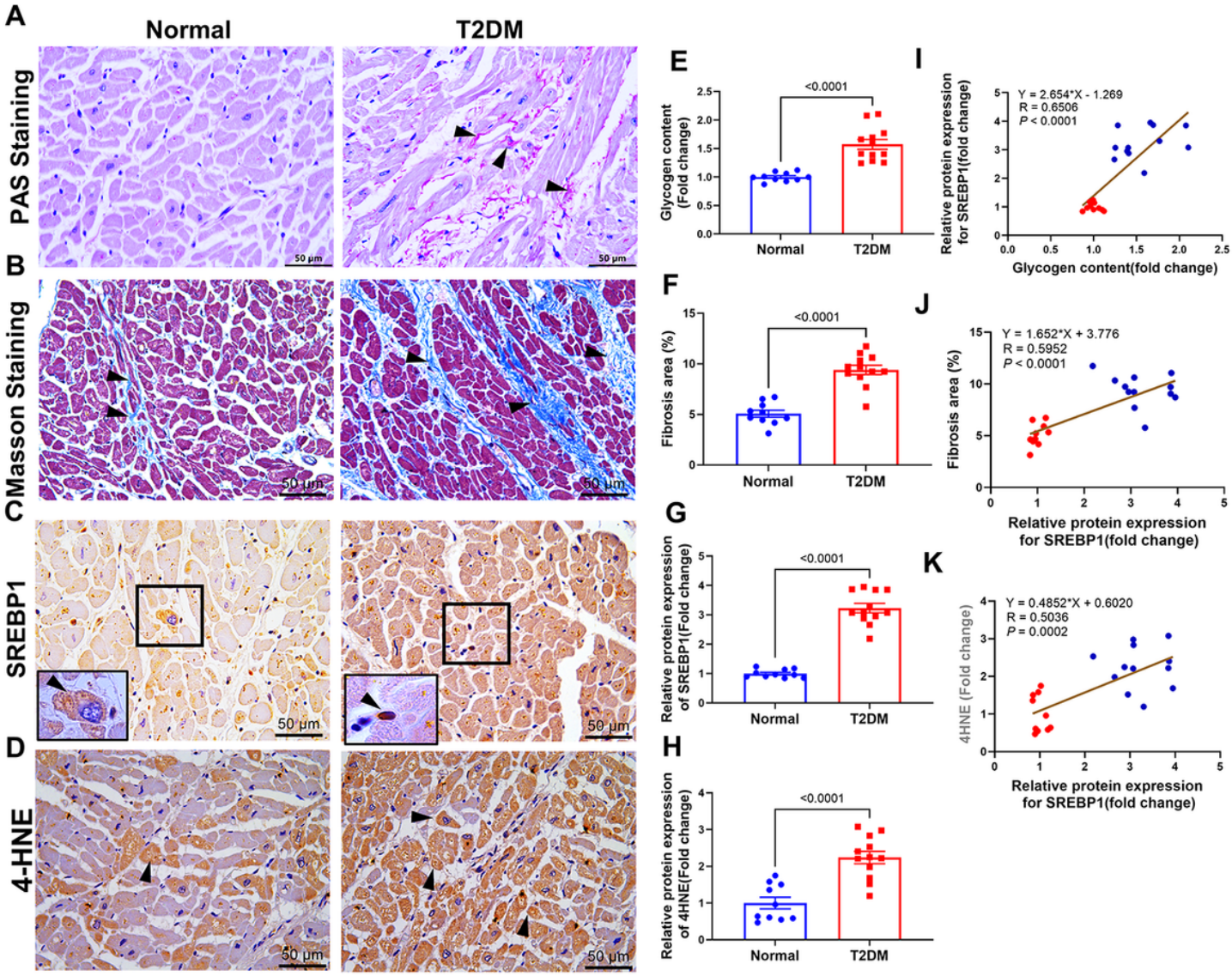

Figure 2

SREBP1 expression positively correlated with cardiac dysfunction in human specimens. (**A-D**) Representative Periodic acid–Schiff (PAS) staining, Masson's trichrome staining, SREBP1

immunohistochemical staining, and 4-HNE immunohistochemical staining immunohistochemical staining images in the myocardium from normal and T2DM patients. Black arrows indicated glycogen deposition (**A**), collagen deposition (**B**), SREBP1 nuclear translocation (**C**), 4-HNE positive expression (**D**) in the myocardium. Original magnification × 400, scale bar = 50 μm. (**E-H**) Quantitative analysis of glycogen, fibrosis, SREBP1 expression, and 4-HNE expression within the myocardium. (**I-K**) Linear correlation analysis. Red dots indicated normal people and blue dots indicated T2DM patients. n = 10 in Normal group, and n = 12 in T2DM group. Data are expressed as means ± SEM. A two-tailed unpaired Student t-test was used for analysis in (**E–H**). For correlation analysis, linear regression models were performed and the goodness of fit for regression models was assessed using R values.

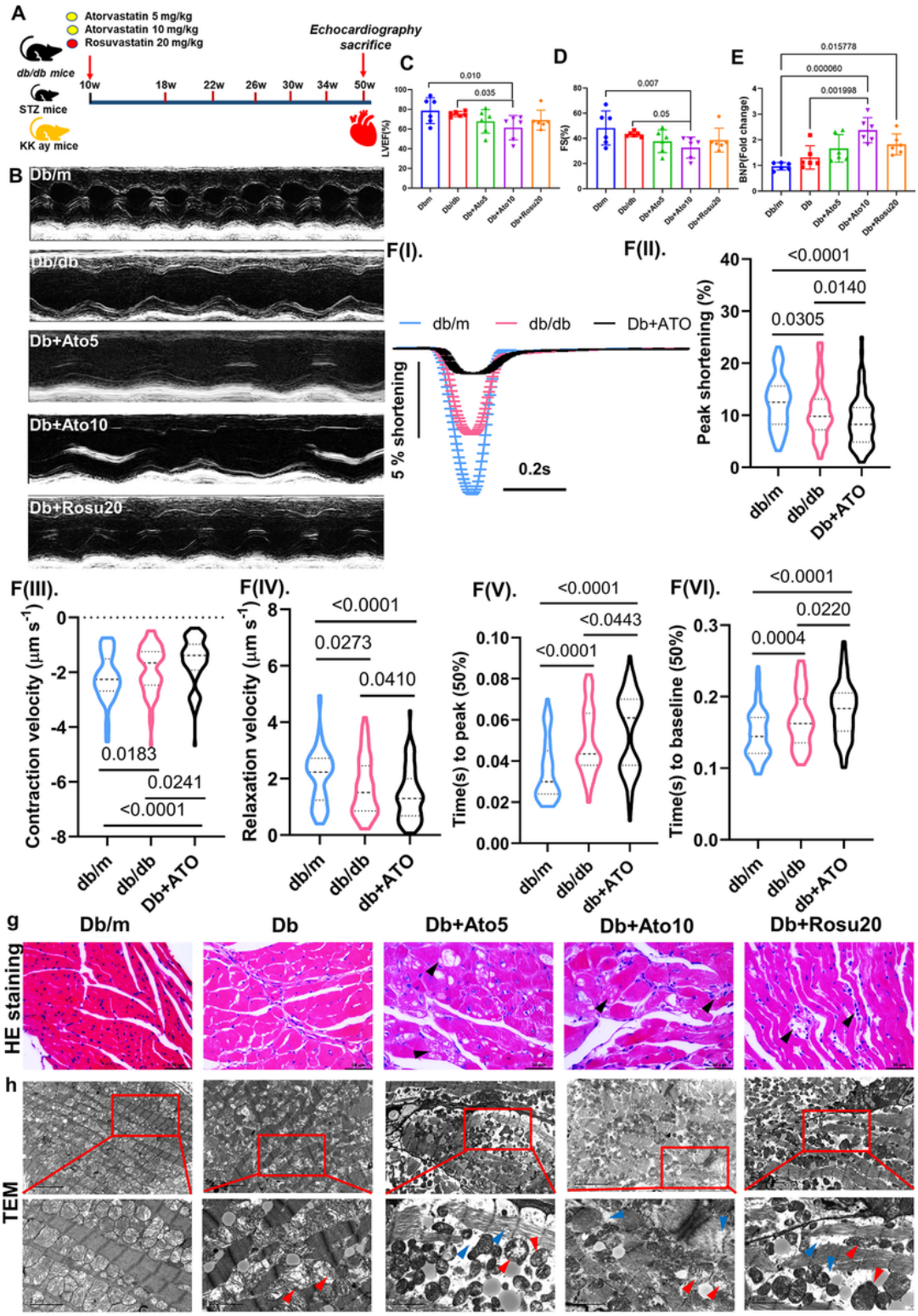

Figure 3

Long-term statins administration worsens diabetes-induced cardiac dysfunction and pathological remodeling. **(A)** Schematic diagram showing the procedure of long-term administration of statins for *db/db* mice. **(B)** Representative left ventricular M-mode echocardiographic tracings from each group of *db/db* mice. **(C-D)**Quantification of ejection fraction, fractional shortening. *n* = 6 in each group. **(E)** Detection of BNP in serum in statins-treated *db/db*mice. **(F)** Cardiomyocyte contractility assay. *n* = 3 in

each group. (**F-I**) Representative sarcomere shortening. (**F-II**) Peak shortening. (**F-III**) Contraction velocity. (**F-IV**) Relaxation velocity. (**F-V**) Time(s) to peak (50%). (**F-VI**) Time(s) to baseline (50%). **(G)** Representative HE staining images in the myocardium. Black arrows indicated vacuolar degeneration and inflammatory infiltrate of cardiomyocytes. Original magnification × 400, scale bar = 50 μm. **(H)** Representative TEM images in the myocardium. Red arrows indicated cardiac mitochondrial swelling and condensation; blue arrows indicated myofibril breakage, lysis and necrosis. Original magnification × 8000 or × 20000, scale bar = 5 or 2 μm. Data are expressed as means ± SEM. One-way ANOVA with Tukey post hoc test was used for the analysis of statistical significance.

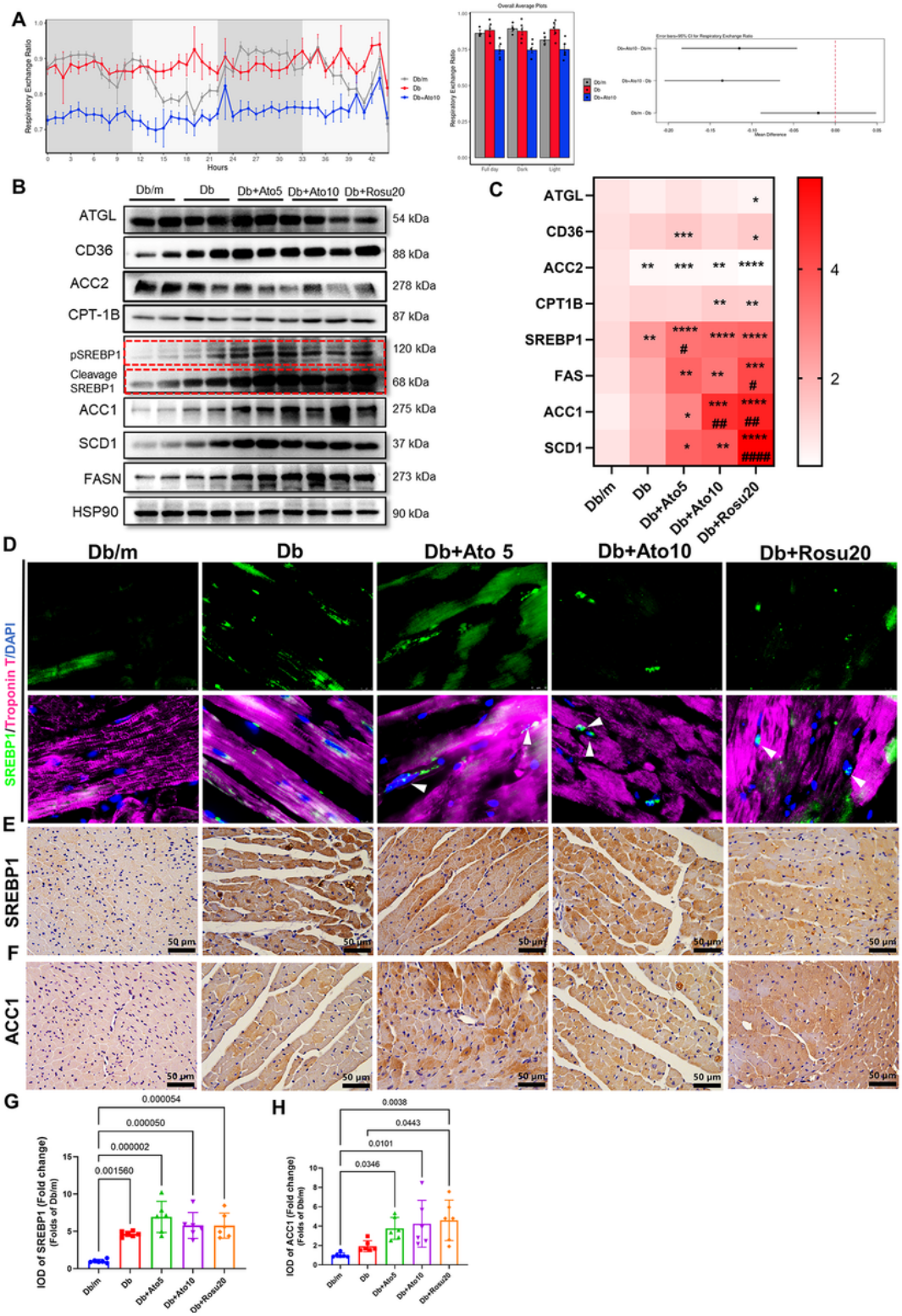

Figure 4

SREBP1 lipogenesis pathway as a central players of statins-induced cardiac lipid metabolism disorder. **(A)**Respiratory exchange ratio (RER) of *db/db* mice after statins-treated at the end of the study. *n* = 5 in each group. **(B-C)** Representative immunoblot images and quantification of ATGL, CD36, ACC2, SREBP1, ACC1, SCD1, FASN in the heart tissues. HSP90 was used as an internal control. **(D)** Immunofluorescence staining of protein SREBP1(green) and cardiomyocyte marker Troponin T(pink) in the myocardium. White

arrows indicated SREBP1 nuclear translocation. Original magnification × 1000, scale bar = 20 μm. **(E-F)** Immunohistochemistry staining of SREBP1 and ACC1 of heart from each group of *db/db*mice. Original magnification × 400, scale bar = 50 μm. **(G-H)**Analysis of SREBP1 and ACC1 protein expression in the myocardium according to immunohistochemical staining. *n* = 6 in each group. Data are expressed as means ± SEM. One-way ANOVA with Tukey post hoc test was used for the analysis of statistical significance.

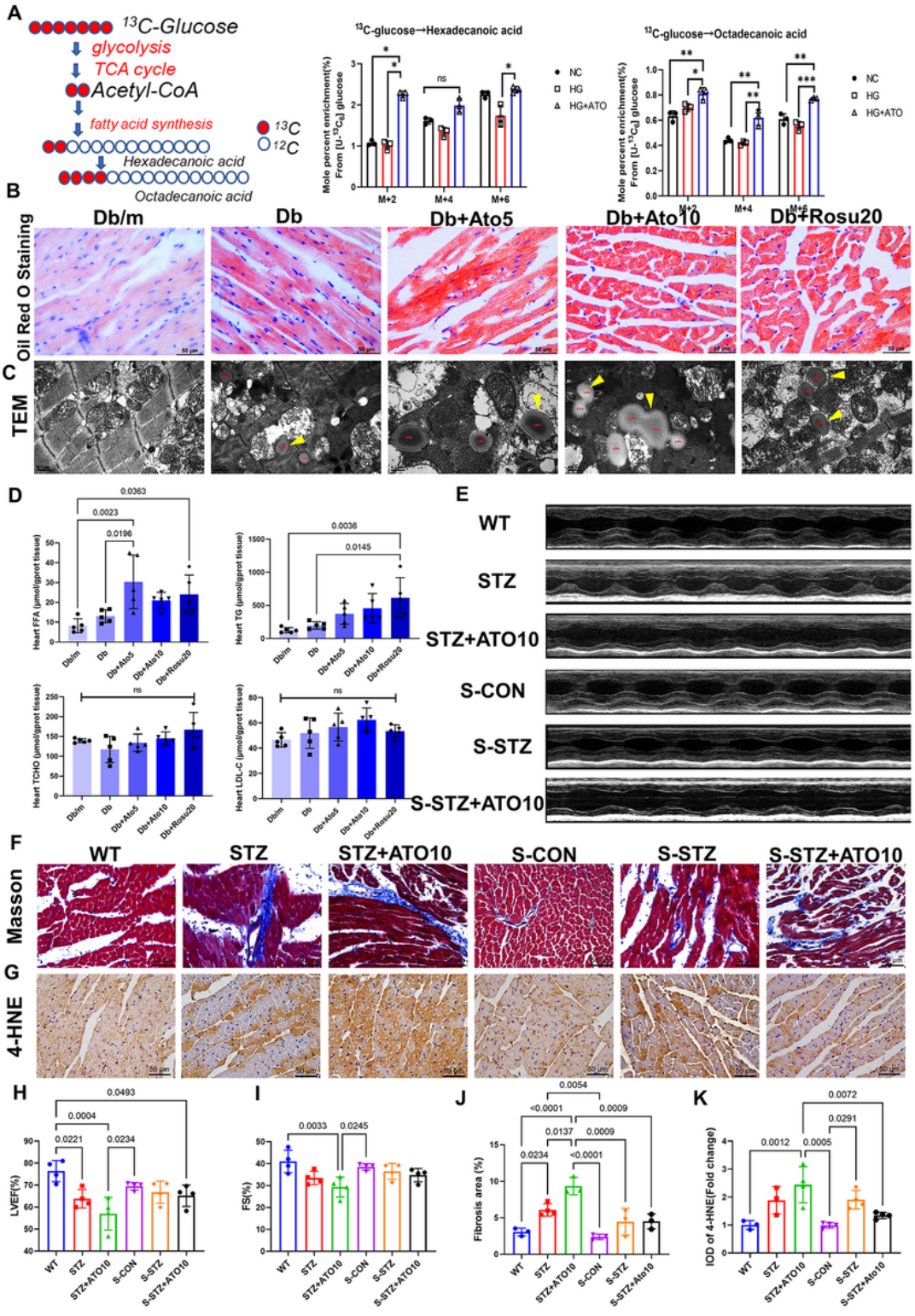

Figure 5

Genetic knock down of SREBP1 alleviated statins-induced cardiac dysfunction. (A) Metabolic flux analysis of atorvastatin treated NMPCs labeled by ^{13}C-glucose that is utilized for the de novo fatty acid synthesis (left panel). The incorporation of ^{13}C into Hexadecanoic acid and Octadecanoic acid were shown in the middle and right panels. **(B)** Representative Oil-red O staining images in the myocardium. **(C)** Representative TEM images of left ventricular walls of the hearts from each group of *db/db* mice. LDs indicated lipid droplets. Yellow arrows represent lipid droplets deposited in cardiomyocytes. Scale bar = 0.5μm. **(D)** Determination of cardiac tissue TCHO, LDL-C, TG and FFA contents from each group of *db/db* mice. *n* = 5 in each group. **(E)** Representative left ventricular M-mode echocardiographic tracings from each group of STZ-induced diabetic mice. S-CON indicated *srebp1* deficient mouse. S-STZ indicated STZ-induced diabetic mice of *srebp1* deficient mouse. S-STZ+ATO10 indicated *srebp1* deficient diabetic mouse atorvastatin treated for 30weeks. **(F-G)** Representative Masson's trichrome staining, 4-HNE (IHC) images of left ventricular walls of the hearts from each group of STZ-induced diabetic mice. Original magnification × 400, scale bar = 50 μm. **(H-I)** Quantification of ejection fraction, fractional shortening. *n* = 4 in each group. **(J)** Semiquantification analysis of fibrotic areas in the myocardium. **(K)** Semiquantification analysis of 4-HNE expression in each group. *n* = 4 in each group. Data are expressed as means ± SEM. One-way ANOVA with Tukey post hoc test was used for the analysis of statistical significance.

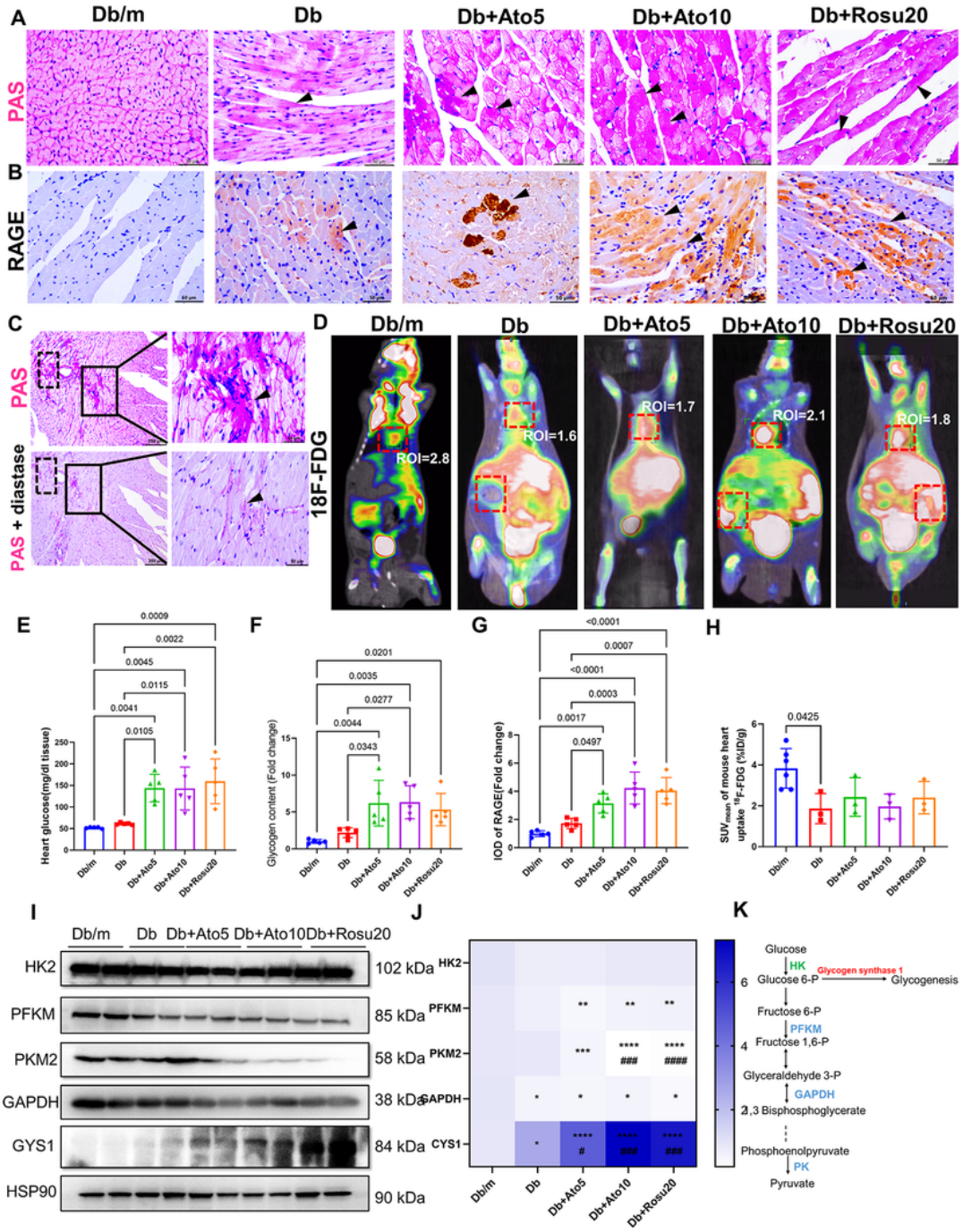

Figure 6

Increased cardiac glucose accumulation may be a contributing factor to statins-induced abnormal activation of SREBP1. (A-B) Representative PAS staining and RAGE immunohistochemical staining images of left ventricular walls of the hearts from each group of *db/db* mice. Black arrows indicated glycogen deposition (A), RAGE positive expression (B). **(C)** Heart sections were treated with diastase as negative control of PAS staining. Original magnification × 400, scale bar = 50 μm. **(D)** Representative

images of ^{18}F-FDG PET/CT from each group of *db/db* mice. **(E)** Determination of cardiac tissue glucose contents from each group of *db/db* mice. **(F)** Analysis of glycogen content in heart according to PAS staining. **(G)** Analysis of RAGE protein expression in the myocardium according to immunohistochemical staining. n = 5 in each group. **(H)** SUV_{mean} of mouse heart uptake ^{18}F-FDG. n = 3 in each group. **(I)** Representative immunoblot images of HK2, PFKM, PKM2, GAPDH, and GYS1 in the heart tissues. HSP90 was used as an internal control. **(J)** Quantification of HK2, PFKM, PKM2, GAPDH, and GYS1 protein expression in the myocardium according to immunoblot. n = 6 in each group. **(K)** Schematic diagram showing the glycolysis related enzymes changing of long-term administration of statins for *db/db* mice. Data are expressed as means ± SEM. One-way ANOVA with Tukey post hoc test was used for the analysis of statistical significance.

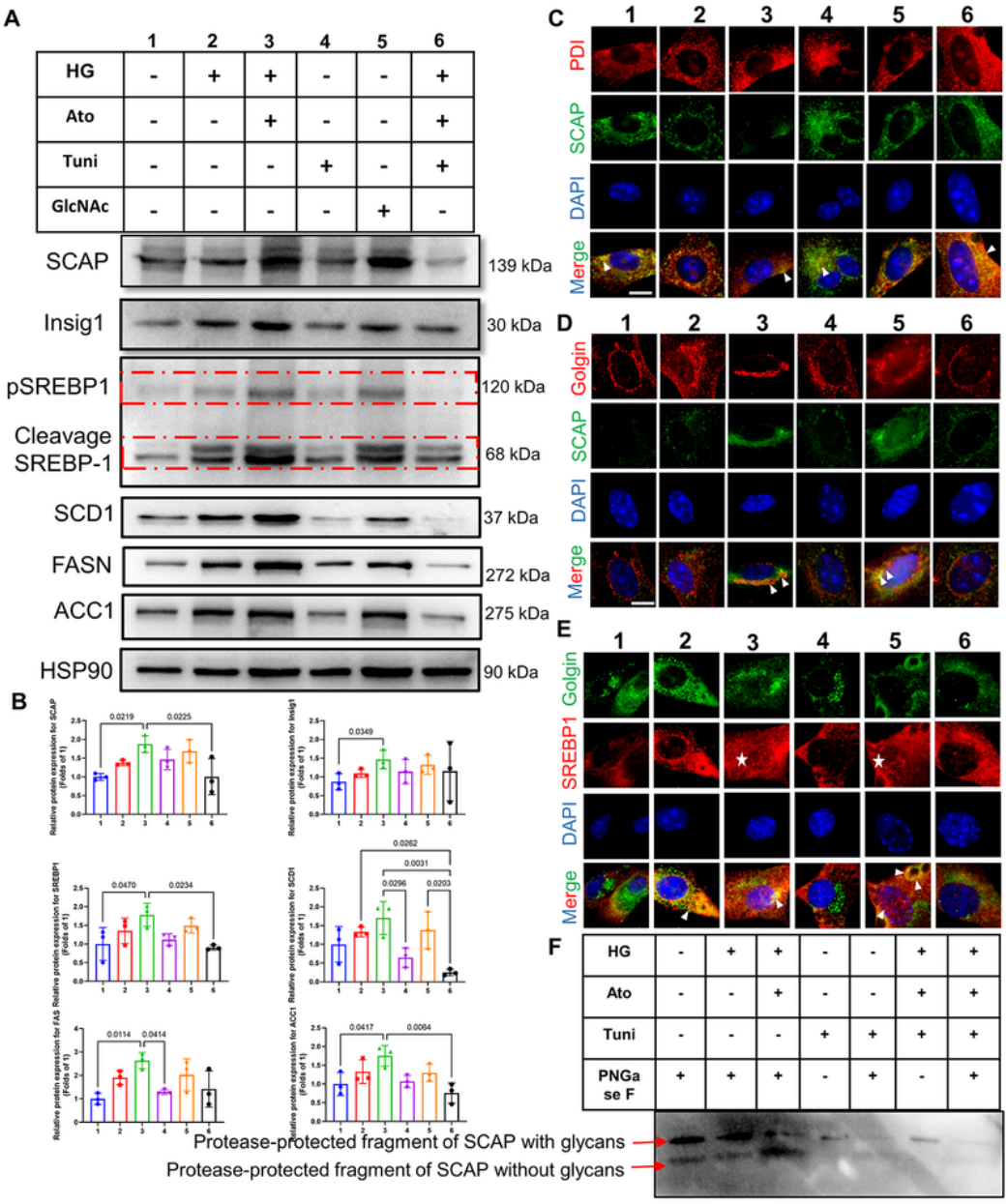

Figure 7

Statins via enhancing intracellular accumulation of glucose promotes SCAP N-glycosylation and trafficking to the Golgi leading to SREBP-1. NMPCswere subjected to starvation in a serum-free medium overnight, then divide into 6 groups, respectively cultured in glucose 1.0 mmol/l (group 1), cultured in a glucose 4.5 mmol/l (group 2), the group 3 treated with glucose 4.5 mmol/l and atorvastatin10 mmol/l, the group 4 treated with tunicamycin (1 μg/ml), the group 5 treated with GlcNAc (20 mM), the group 6

treated with glucose 4.5 mmol/l and atorvastatin10 mmol/l, tunicamycin (1 μg/ml). All groups NMPCs were cultured for 24 hours. **(A-B)**Representative immunoblot images and quantification of SCAP, insig1, SREBP1, SCD1, FASN, and ACC1. HSP90 was used as an internal control. The demonstrated bands were typical from 3 experimental repeats. **(C)** Immunofluorescence images of SCAP (green) sub-cellular localization in relation with the Endoplasmic reticulum protein marker Protein disulfide-isomerase (PDI) (red) and nuclear DAPI staining (blue) in NMPCs with same treatment procedure as panel a. White arrows indicated merged SCAP and PDI signals (yellow). **(D)** Immunofluorescence images of SCAP (green) sub-cellular localization in relation with the Golgi protein marker Golgin (red) and nuclear DAPI staining (blue) in NMPCs with same treatment procedure as panel a. White arrows indicated merged SCAP and Golgin signals (yellow), which meant translocation of endogenous SCAP into the Golgi. **(E)** Immunofluorescence images of SREBP1 (red) sub-cellular localization in relation with the Golgi protein marker Golgin (green) and nuclearDAPI staining (blue) in NMPCs with same treatment procedure as panel a. White stars indicated translocation of endogenous SREBP1 into the nucleus, white arrows indicated merged SREBP1 and Golgin signals (yellow). Original magnification × 1000, scale bars=20 μm. **(F)** N-glycans of SCAP were analyzed as described in the Supplementary materials and methods section. Data are expressed as means ± SEM. One-way ANOVA with Tukey post hoc test was used for the analysis of statistical significance.

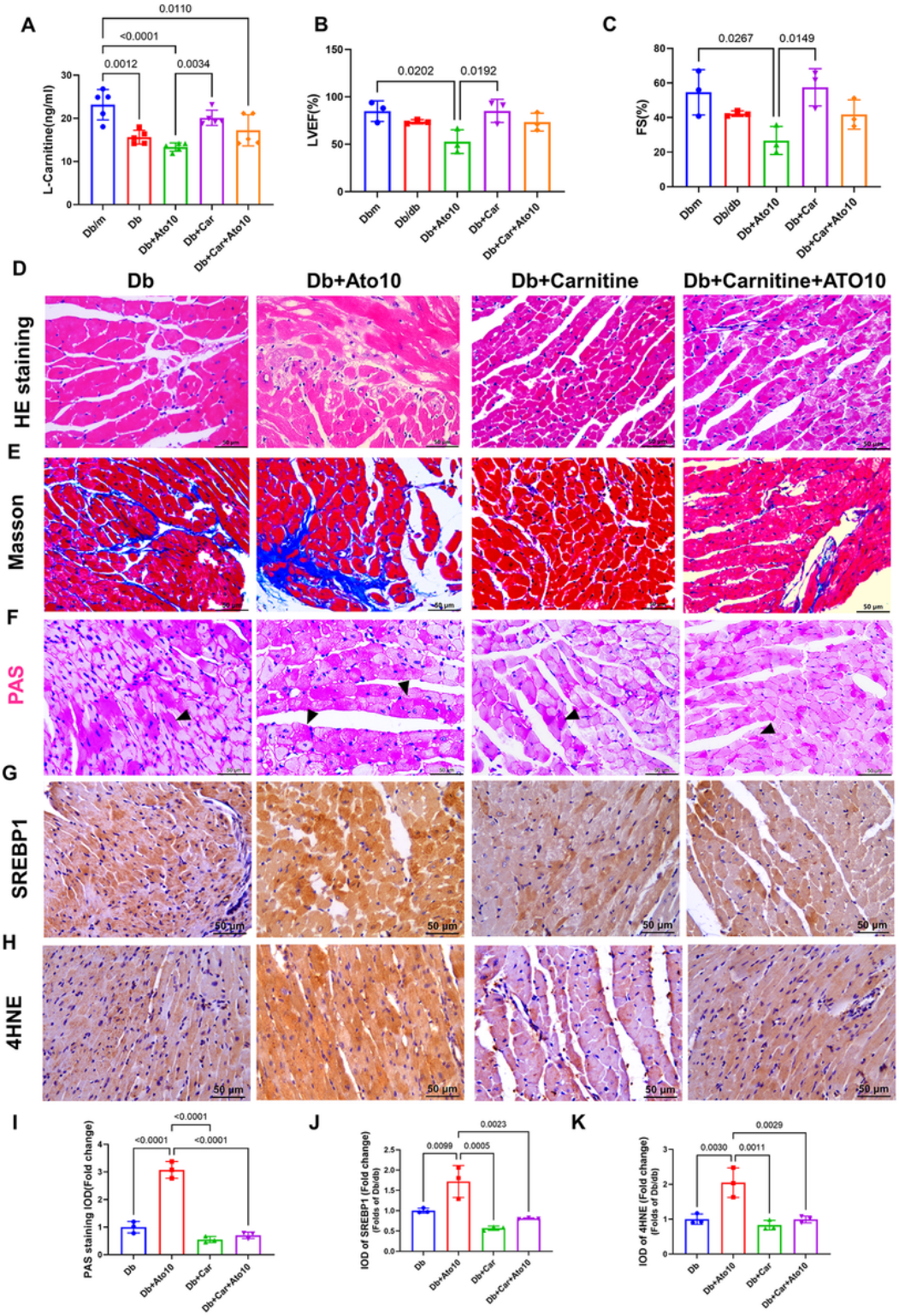

Figure 8

Statin combined with L-carnitine alleviates cardiac dysfunction and pathological remodeling. **(A)**Detection of L-carnitine content in heart tissue. *n* = 5 in each group. **(B-C)** Quantification of ejection fraction, fractional shortening of left ventricular M-mode echocardiographic tracings. *n* = 3 in each group. **(D-H)** Representative HE staining, Masson's trichrome staining, PAS staining, SREBP1 staining and 4HNE staining images of heart sections. **(I-K)** Semiquantification analysis of PAS staining, SREBP1 staining

and 4HNE staining. *n* = 3 in each group. Data are expressed as means ± SEM. One-way ANOVA with Tukey post hoc test was used for the analysis of statistical significance.

Supplementary Files

This is a list of supplementary files associated with this preprint. Click to download.

- SupplementaryMaterials.docx